Biaxial strain-modified valence and conduction band offsets of zinc-blende GaN, GaP, GaAs, InN, InP, and InAs, and optical bowing of strained epitaxial InGaN alloys

Biaxial strain-modified valence and conduction band offsets of zinc-blende GaN, GaP, GaAs, InN, InP, and InAs, and optical bowing of strained epitaxial InGaN alloys

P. R. C. Kent, Gus L. W. Hart, and Alex Zunger[a)]

National Renewable Energy Laboratory, Golden, Colorado 80401

Using density-functional calculations, we obtain the (001) biaxial strain dependence of the valence and conduction band energies of GaN, GaP, GaAs, InN, InP, and InAs. The results are fit to a convenient-to-use polynomial and the fits provided in tabular form. Using the calculated biaxial deformation potentials in large supercell empirical pseudopotential calculations, we demonstrate that epitaxial strain reduces the InGaN alloy bowing coefficient compared to relaxed bulk alloys. © *2002 American Institute of Physics.* [DOI: 10.1063/1.1524299]

The energy of the conduction band minimum (CBM) and valence band maximum (VBM) of common zinc-blende semiconductors can be altered[1] via hydrostatic pressure,[2] epitaxy-induced biaxial strain,[3–6] or alloying.[7] These energy changes are important parameters needed for the quantum design of electronic nanostructures. The rate of change of CBM and VBM energies with hydrostatic pressure ("absolute pressure deformation potentials") is summarized in Ref. 2 for many common binary semiconductors. However, reliable absolute *biaxial* deformation potentials are less common (e.g., Refs. 4 and 6). Here, we provide easy to use, fitted numerical results of the variation with (001) strain of the VBM and CBM energies of zinc-blende GaN, GaP, GaAs, InN, InP, and InAs, obtained from first-principles local-density calculations.

The VBM of zinc-blende materials consists of degenerate bands (two-fold Γ_{8v} and one-fold Γ_{7v}) and, therefore, their response to strain is complex.[8] Previously, first-order, linear in strain, perturbation models within the envelope function approximation have been used.[3,7] Here, we calculate the band structure of each strained system self-consistently, so our results are not limited to small strains, envelope function approximations, or to low-order perturbative treatments of the strain-mediated interband coupling. Once obtained, the VBM and CBM energies are fit to a low-order polynomial in strain. Together with the InX/GaX (X=N,P,As) *unstrained* valence band offset (tabulated in Ref. 9 for all common semiconductors), our results give the band offsets between InX/GaX at any intermediate (001) strain (i.e., corresponding to a substrate with in-plane lattice constant between that of InX and GaX).

The band structure and tetragonal deformations of strained zinc-blende materials were calculated in the local-density approximation using the linear augmented plane wave (LAPW) approach[10,11] (*WIEN*97 implementation),[12] including spin–orbit effects. We use the exchange correlation of Perdew and Wang.[13] For each in-plane (001) lattice constant $a_{InX} \leq a_{\text{in-plane}} \leq a_{GaX}$, we minimize the total energy with respect to the tetragonal distortion c/a. The band structure is then computed at $[a_{\text{in-plane}}; (c/a)_{\text{eq}}]$ for a range of

$a_{\text{in-plane}}$ values. To separate the movement of the VBM and CBM, we use the energy of the lowest $1s$ states as a reference. (This is similar to both the experimental photoemission spectroscopy approach[14,15] and first-principles calculational approach[16] to determining band offsets.) Although we use the local-density approximation for the conduction states, which are subject to the band gap error, we expect the *change* in the conduction state energies with lattice constant to be accurate.

The results for InP/GaP are plotted in Fig. 1 where we have aligned the unstrained eigenvalues using the *calculated* valence band offset[9] and the unstrained *experimental* band gaps.[17] Results are fit to polynomials of the form

$$E_{SO} = \Delta_{so} + C_1 x + C_2 x^2 + C_3 x^3, \qquad (1)$$

$$E_{HH} = C_1 x + C_2 x^2 + C_3 x^3, \qquad (2)$$

$$E_{LH} = C_1 x + C_2 x^2 + C_3 x^3, \qquad (3)$$

$$E_{CBM} = E_{gap} + C_1 x + C_2 x^2 + C_3 x^3, \qquad (4)$$

where $x \equiv (a_{\text{epi}} - a_0)$, a_{epi} is the in-plane lattice constant, a_0 is the cubic equilibrium lattice constant (in Å), Δ_{so} is the spin–orbit splitting at the VBM interaction, and E_{gap} is the band gap (in eV). This form for the band-edge states gives
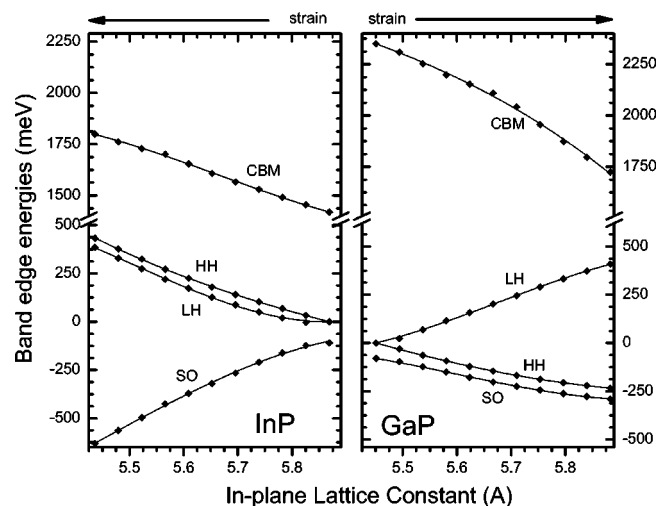

FIG. 1. LAPW calculated CBM and VBM states (indicated by points) for cubic GaP and InP for substrate lattice constants $a_{GaP} \leq a_{\text{in-plane}} \leq a_{InP}$. The corresponding fits from Table I are shown by solid lines.

[a)]Electronic mail: azunger@nrel.gov

are quantitatively similar to Bellaiche *et al.*[19] except for improved statistics in the present work. The strong upward shift of the VBM for indium concentrations <10% is consistent with recent x-ray measurements.[20] In Fig. 5(b), we show the band gap bowing coefficient assuming a gap of 1.9 eV for InN. We see that the bowing coefficient is composition dependent and is large and positive, $\geq$4 eV, for indium compositions below 10%, due to the strong upward bowing of the VBM. For higher indium compositions, the bowing is reduced to 2–3 eV. When we assume in our pseudopotential fit that InN has a gap of 0.8 eV, the bowing coefficient is reduced significantly for both bulk and epitaxial film but the *relative* bowing is unchanged.

To model the epitaxial alloy grown on GaN, we confined the in-plane lattice constant of the $In_xGa_{1-x}N$ alloy to that of GaN, relaxing the c/a ratio and all atomic positions. The band-edge energies, obtained using the same method as for the bulk alloys, are shown in Fig. 5(a) as dashed lines. Now the bowing coefficients are reduced, compared to the bulk, for indium compositions up to ~30%, e.g., $b=2.8$ versus 3.4 eV for the epitaxial and bulk bowing coefficient at $x=0.20$. In Ref. 21, a reduction in bowing coefficient due to expitaxy of 0.7 eV was measured for $x<0.25$.

To understand the effect of epitaxy-reduced alloy bowing, we refer again to Fig. 4. We see that compressing InN biaxially to the in-plane lattice constant of GaN raises the VBM energy by 480 meV and also raises the CBM by 350 meV, so the epitaxial gap is only 130 meV lower than the bulk InN gap. At the other end of the composition range, $x=0$, the bulk and epitaxial gaps are identical. As the In composition increases from $x=0$, the epitaxial alloy reduces its band gap by a lesser amount than the bulk alloy since the GaN component has a *higher* VBM, while the InN component has a *lower* VBM with increasing $a_{\text{in-plane}}$. On the other hand, the CBM of both the GaN and InN components decrease as $a_{\text{in-plane}}$ increases. However, the CBM of the bulk alloy decreases faster than that of the epitaxial alloys. *Consequently, the epitaxial alloy has a smaller optical bowing than the bulk alloy*. This observation shows that larger bow-

ing is expected in relaxed, bulklike samples, while epitaxial samples should have ~0.5 eV lower bowing parameters, for the device-relevant indium composition range of $\leq$30%. This holds for InN gap of either 1.9 or 0.8 eV.